Journal of Applied Remote Sensing

RemoteSensing.SPIEDigitalLibrary.org

Retrieving homogeneous liquid cloud microphysical properties using multiple-field-of-view lidar

Hengheng Zhang
Lingbing Bu
Haiyang Gao
Xingyou Huang
K. Raghavendra Kumar

SPIE.

Hengheng Zhang, Lingbing Bu, Haiyang Gao, Xingyou Huang, K. Raghavendra Kumar, "Retrieving homogeneous liquid cloud microphysical properties using multiple-field-of-view lidar," *J. Appl. Remote Sens.* **12**(4), 046021 (2018), doi: 10.1117/1.JRS.12.046021.

Retrieving homogeneous liquid cloud microphysical properties using multiple-field-of-view lidar

Hengheng Zhang,[a,b] Lingbing Bu,[a,b,c,*] Haiyang Gao,[a,b,c] Xingyou Huang,[a,b,c] and K. Raghavendra Kumar[b]

[a]Ministry of Education (KLME), Collaborative Innovation Centre on Forecast and Evaluation of Meteorological Disasters, Key Laboratory of Meteorological Disaster, China

[b]Nanjing University of Information Science and Technology, School of Atmospheric Physics, Nanjing, Jiangsu, China

[c]International Joint Laboratory on Climate and Environment Change, Key Laboratory for Aerosol-Cloud-Precipitation of China Meteorological Administration, China

Abstract. Liquid water content (LWC) and cloud droplet effective size (CDES) are important factors affecting atmospheric radiative transfer, and measurement of these parameters in clouds is essential. For homogeneous liquid cloud (constant extinction coefficient) with a gamma size distribution of cloud droplets, we find that LWC and CDES can be retrieved from two parameters obtained from a multiple-field-of-view (MFOV) Lidar: the intercept of the range-corrected Lidar signal (IRCLS) and the slope of the range-corrected Lidar signal (SRCLS) at different sizes of FOV. Monte Carlo simulations reveal that IRCLS at different sizes of FOV varies with both extinction coefficient and CDES while SRCLS varies only with the extinction coefficient, which depends on both LWC and CDES. This means that, after extracting the extinction coefficient using SRCLS, we can easily obtain CDES from IRCLS, and LWC can then be determined using the extinction coefficient. An innovative MFOV Lidar system is constructed to measure the LWC and CDES. A series of experiments is conducted in the northern suburb of Nanjing, China, and the LWC and CDES of homogeneous liquid cloud are obtained. Comparisons among results from the MFOV Lidar, theoretical calculation, and the global precipitation measurement satellite verify our proposed method. [DOI: 10.1117/1.JRS.12.046021]

Keywords: multiple-field-of-view lidar; multiple scattering; liquid water content; cloud droplet effective size.

Paper 180352 received Apr. 26, 2018; accepted for publication Oct. 23, 2018; published online Nov. 13, 2018.

1 Introduction

Microphysical properties of clouds, such as liquid water content (LWC) and cloud droplet effective size (CDES), are important factors affecting atmospheric radiative transfer.[1,2] Thus, a variety of methods, categorized as either active or passive methods, are often used to retrieve these parameters.[3] One active method uses a millimeter-wave cloud radar (MWCR) to measure the LWC and CDES. Reflectivity (in units of dBZ) is a data product derived from an MWCR that can be used to retrieve LWC through an empirical relationship formula.[4] However, an MWCR cannot detect thin cloud with small optical depth and the choice of empirical parameters is difficult when considering different types of cloud.[5] When a traditional elastic Lidar is used to detect liquid cloud, it is unlikely to obtain the size spectrum distribution of the liquid cloud.[6] Another method combines Lidar and MWCR, but may be limited because of the different scattering cross-section between Lidar and MWCR.[7] Raman Lidars are also not the best instrument for cloud measurement because of the weak Raman signal and strong background noise, especially in the daytime.[8,9]

*Address all correspondence to: Lingbing Bu, E-mail: lingbingbu@nuist.edu.cn

1931-3195/2018/$25.00 © 2018 SPIE

A method using multiple scattering effects has been proposed to retrieve the microphysical properties of cloud.[10] In the last decade, significant research progress has been made on the influence of multiple scattering effects on Lidar signals. Among them, Platt[11] calculated multiple scattering effects using the Monte Carlo method and first emphasized the importance of multiple scattering for cirrus clouds. Later, Hu et al.[12] used layer integrated depolarization ratios and empirical results to simulate the relationship between the extinction coefficient and the effective radius, using parameters that are physically quite different from each other, such as the exponential decay rate of the liquid cloud attenuated backscatter signal within clouds and the absorption of near-IR radiation at a wavelength of 3.7 μm. Further, Hu et al.[13] and Kim et al.[14] calculated a simple relationship between the degree of depolarization and the multiple scattering contributions of the Lidar signal using Monte Carlo simulations with the assumption that LWC and CDES are constant within clouds. This calculation showed that the degree of linear polarization (DLP) decreases from 1 to 0 as the depth from the cloud base increases. Also, Kim et al.[15] determined the influences of multiple-scattering effects on Lidar signals for different values of CDES and LWC through Monte Carlo simulation based on a homogeneous liquid cloud model. They found a simple correspondence between the water droplet optical depth and the degree of depolarization in a modified gamma size distribution. As suggested by Kim et al.,[15] LWC and CDES can be retrieved from the slope of the DLP at the cloud base and the saturated DLP at an infinite altitude. Donovan et al.[16] also proposed that liquid-cloud microphysical properties can be determined using depolarization Lidar, assuming that the clouds exhibit characteristics of (quasi-)linear LWC profiles and (quasi-) constant cloud-droplet number density in the cloud base region. Although substantial progress has been made on theoretical studies of multiple scattering, to the best of our knowledge, very little experimental research has been conducted.

Unlike traditional Lidar, which generally has a fixed and small FOV, collecting signals from multiple scattering is difficult because the light from multiple scattering may cause off-tracking of 180 deg. To overcome this issue, a multiple-field-of-view (MFOV) Lidar was proposed to collect multiple scattering signals.[17] The MFOV Lidar can collect signals with different sizes of FOV and retrieve the microphysical properties of cloud.

In this study, we propose a method for measuring LWC and CDES parameters using MFOV Lidar. First, Lidar signals under different conditions are calculated using a Monte Carlo simulation to determine how the Lidar signals reflect the microphysical properties of cloud. It is shown that the LWC and CDES can be obtained from the intercept of the range-corrected Lidar signal (IRCLS) and the slope of the range-corrected Lidar signal (SRCLS) using MFOV Lidar. Further, we constructed an MFOV Lidar system with a variable concentric pinhole to observe liquid cloud signals in the northern suburb of Nanjing, East China; the results from this Lidar system are compared with those from the theoretical calculation and Global Precipitation Measurement satellite (GPM), which verifies our proposed method.

2 Method for Retrieving LWC and CDES Using MFOV Lidar

The Monte Carlo method provides effective and practical simulations of multiple scattering. This method is used to track the random walk of a large number of photons in the medium to obtain the scattering characteristics of light according to statistical laws. For the tracking of photons, it is necessary to sample the step size of the random walk and scattering angle. According to sampling principles, the step size of the random walk can be evaluated as: $s = \ln \xi/\sigma$, where ξ is a random number from 0 to 1, and σ is the extinction coefficient. The specific steps are as follows:

1. Photon state initialization: incident direction initialization and polarization state initialization.
2. Photon projection: based on the step size of the random walk(s), judge whether the photons are in the clouds or not. If a photon escapes from the clouds, retrack the next photon.
3. Photon scattering: if the photons are in the cloud then the light will be scattered after colliding with cloud droplets. The scattering energy can be divided into two parts: one part is directly scattered to the Lidar receiver based on analytical probability; the other part continues to scatter within the cloud until it escapes.

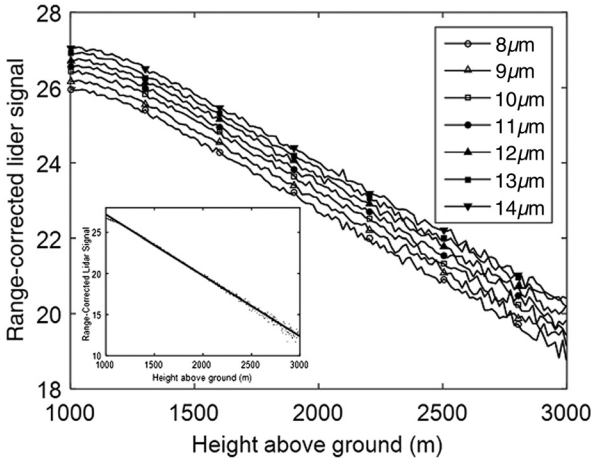

Fig. 1 RCLS versus distance from the ground for different CDES values with extinction coefficient, FOV, LBD, cloud base (CB), and cloud top (CT) values of 2 km^{-1}, 2 mrad, 1 mrad, 1000 m, and 3000 m, respectively. Inset: typical plot of the RCLS versus distance from the ground for given cloud parameters. (CB = 1000 m, CT = 3000 m, extinction coefficient = 2 km^{-1}, CDES = 8 μm, FOV = 2 mrad, and LBD = 1 mrad).

The cloud model used in this research is a simple but useful model of cloud-base conditions; numerous researchers have used this cloud model to study multiple scattering effects on clouds as shown in Refs. 14, 15, and 18. We assume that the cloud is homogeneous and the liquid cloud droplet size follows a gamma distribution.[18] Based on the Monte Carlo method, we carried out simulations of multiple scattering in the cloud. Figure 1 shows the calculated Lidar echo signals with laser light wavelength, laser beam divergence (LBD), and FOV of 532 nm, 1 mrad, and 2 mrad, respectively.

The inset in Fig. 1 shows the definitions of SRCLS and IRCLS used in this study, with a logarithmic range-corrected Lidar signal (RCLS). SRCLS is defined as the slope of the fitted line, while IRCLS is defined as the intercept of the fitted line, both of which can be determined from the linear fitting using the least squares method. Figure 1 shows the variation of RCLS as a function of distance from the ground for different values of CDES with a constant extinction coefficient (refer to multiple-scattering extinction coefficient if not particularly point out). The LIDAR FOV, LBD, laser wavelength, and CB were 2 mrad, 1 mrad, 532 nm, and 1000 m, respectively. It is evident that IRCLS varies with CDES, and SRCLS is independent of CDES when the extinction coefficient is constant. This means that the extinction coefficient can be extracted from the values of SRCLS, which contains no information about CDES.

Figure 2(a) shows SRCLS versus CDES for different values of extinction coefficient for the given CB, FOV, and LBD. SRCLS is almost constant for a constant extinction coefficient. According to the slope method,[19] which only considers single scattering, the extinction coefficient and SRCLS satisfy the following linear relationship:

$$\begin{cases} \alpha(z) = -\frac{1}{2}\frac{dD(z)}{dz} = -\frac{1}{2}\mathrm{SRCLS} \\ D(z) = \ln[P(z)\cdot z^2] \end{cases}, \tag{1}$$

where $P(z)$ is the Lidar signal at different heights and z is the height or distance from the ground.

As for multiple scattering, we can use the multiple scattering factor η to correct the extinction coefficient. Here, η represents the degree of multiple scattering. Outside the cloud, η is assumed to be 1; inside the cloud, Winker[20] found that the multiple scattering factor η can be calculated as follows:

$$\begin{cases} \eta(z) = 1 - \frac{\ln(\mathrm{MMS})}{2\delta(z)} \\ \delta(z) = -\int_0^z \alpha(z)\mathrm{d}z \end{cases}, \tag{2}$$

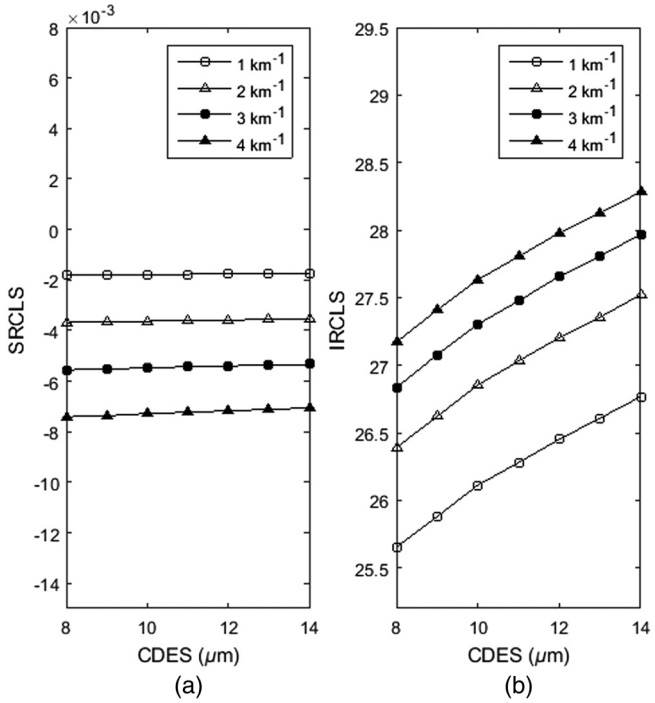

Fig. 2 (a) SRCLS and (b) IRCLS versus CDES for different extinction coefficient values. The FOV, LBD, and CB are 2 mrad, 1 mrad, and 3000 m, respectively.

where MMS represents the ratio of multiple (total) scattering and single scattering, which can be calculated using the Monte Carlo method, and α is the single scattering extinction coefficient.

Figure 2(b) shows IRCLS versus CDES for different extinction coefficients with fixed values of FOV, LBD, and CB. IRCLS varies strongly not only with extinction coefficient but also with CDES. This indicates that, after extracting the extinction coefficient from the SRCLS value, we can gradually obtain CDES from the IRCLS value. Both SRCLS and IRCLS can be measured using single wavelength MFOV Lidar.

However, when considering multiple scattering factor η, extinction coefficient depends on SRCLS and multiple scattering factor η. Different multiple scattering factors at different sizes of FOV cause different SRCLS and IRCLS. According to Fig. 2, SRCLS does not have an obvious relationship with CDES while IRCLS varies strongly with CDES and extinction coefficients, which means that IRCLS is more sensitive to multiple scattering factor than SRCLS. However, as for this method applied in MFOV Lidar system, multiple scattering factor has influence on the retrieve results as constant SRCLS does not mean constant extinction coefficient when multiple scattering factor has change a lot at different sizes of FOV. So the interval of FOVs cannot be too lager in the reality observation in order to multiple scattering factor remained constant at different sizes of FOV. Also, the averaged multiple scattering factors for different values of FOVs (1, 1.5, 2, and 2.5 mrad) with the LBD being 1 mrad are 0.9589, 0.9517, 0.9424, and 0.9325, respectively. So the multiple scattering factors almost maintain constant with the size of FOV changing 0.5 mrad, which means that the differences caused by multiple scattering factor can be ignored if the interval of different FOVs is smaller than 0.5 mrad.

From the aforementioned calculation, we proposed a method to retrieve LWC and CDES using MFOV Lidar. First, SRCLS and IRCLS can be calculated from the Lidar signal, which is collected at different values of FOV. Second, the cloud particle extinction coefficient can be obtained from SRCLS, which has no relationship with CDES. After the extinction coefficient is determined, CDES can be retrieved from IRCLS at different fields of view, which vary with both extinction coefficient and CDES. Finally, LWC can be calculated from the extinction coefficient as CDES is already known. The flowchart of this method is shown in Fig. 3.

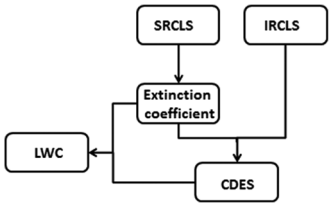

Fig. 3 Flowchart of the retrieval method.

3 Construction of MFOV Lidar System

To measure LWC and CDES using the aforementioned method, we constructed an MFOV Lidar system by placing an automatic electrical pinhole on the focal plane of the receiving telescope. The schematic diagram of this MFOV Lidar is shown in Fig. 4. The Lidar system employs a compact Nd:YAG laser as the light source, which generates a second harmonic at 532 nm. The repetition rate and pulse energy of the laser are 1 KHz and 100 μJ, respectively. The LBD is compressed to 0.4 mrad by an adjustable beam expander. The laser is reflected into the atmosphere by a 45-deg mirror. The backscattered laser is collected by a Cassegrain telescope with a focal length of 2000 mm. After being collimated and filtered, the collected scattered light is detected by a photomultiplier tube (PMT) which has the function of monitoring whether the signal is saturated or not. Then, the backscattered light is converted to an electrical signal by the PMT, which can be acquired and recorded by the photon counter card. The photon counter card has a count rate of 200 MHz and a variable bin length. The smallest bin length is 100 ns, corresponding to a range solution of 15 m.

We used an automatic electrical pinhole to change the FOV of this Lidar. The pinhole size can be adjusted from 0.5 to 7.0 mm with a minimum step of 50 nm. We achieved synchronization of the photon counting card and the pinhole through LabVIEW software. The accumulative time, step size of the automatic variable pinhole, and the number of steps in each group can be set and controlled by our software. In order to avoid the cumulative error of reciprocating positioning of

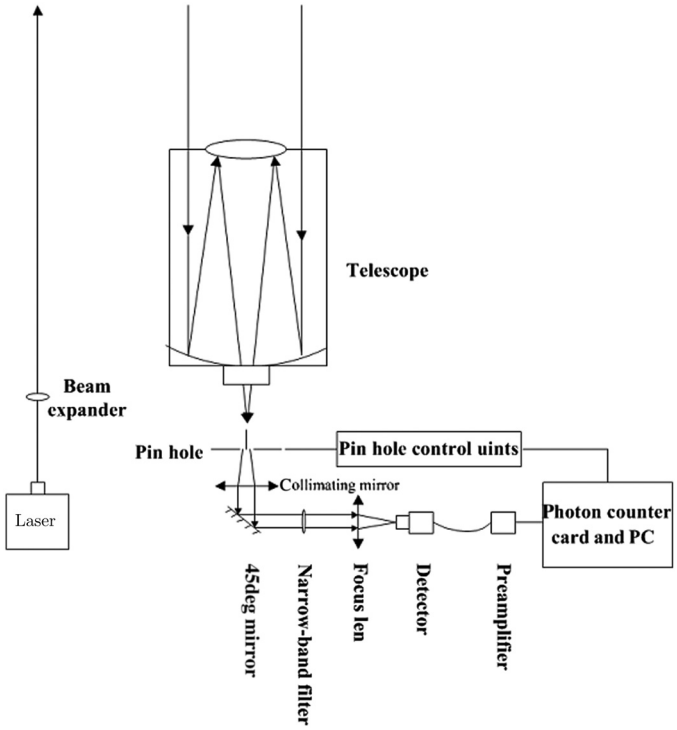

Fig. 4 Schematic diagram of MFOV Lidar.

Table 1 Key parameters and specifications of MFOV Lidar.

Characteristic parameter	Value	Manufacturers
Laser transmitter		Shanghai Brillouin laser technology
Laser	Nd:YAG	
Wavelength	532 nm	
PRF	1 kHz	
Pulse energy	100 μJ	
Beam expander Receiving and detecting	10× adjustable	Thorlabs
Telescope	Cassegrain	Celestron
PMT	H10682-110	Hamamatsu
Filter CWL	532 ± 0.05	Barr associates
Bandwidth	0.2 nm	
Peak transmission	70%	
Signal acquisition Multichannel analyzer	P7882	Fast ComTec
Count rates	200 MHZ	
Pinhole size	0.5 to7.0 mm	SmarAct GmbH

the pinhole, we reset the electric pinhole position at the end of each group. The key parameters and detailed specifications of the MFOV Lidar system are given in Table 1.

4 Liquid Cloud Observations by MFOV Lidar

We made a series of observations in the north suburb of Nanjing from September 2016 to January 2017 using the MFOV Lidar system. Most of the observations were of the liquid cloud. The LBD and vertical resolution were 0.4 mrad and 15 m, respectively. The Lidar integration time for each FOV was 18 s; each data set (three profiles) is acquired within a short period of time (54 s) to avoid effects from significant changes in the cloud at different sizes of FOV. The size of the electric hole was set at 1, 1.5, and 2 mm, corresponding to an FOV of 0.5, 0.75, and 1.0 mrad, respectively. Based on the observed data, cases meeting the criterion of the homogeneous liquid model, which has constant SRCLS, were chosen for further study of cloud microphysical properties. Figure 5 shows the Lidar signal for different sizes of FOV, which was acquired on December 24, 2016. Values of CB and CT were 1965 and 2280 m, respectively (as shown in the black rectangular box); hence, we extracted data in this range for further study of cloud microphysical properties. The inset shows RCLS versus distance from the ground for different values of FOV on a logarithmic scale at heights between 1965 and 2280 m. By means of our calculation, the linear correlation coefficient between RCLS and range is 0.986 at these heights. So we can conclude that although IRCLS varies with FOVs, whereas SRCLS is almost constant for different sizes of FOV. This means that the extinction coefficient is constant; thus, it can be obtained using the slope method.

Figure 6 shows extinction coefficient retrieval from SRCLS. We first calculated the extinction coefficient using the slope method for different sizes of FOV. In this figure, the dotted line indicates observed data and the solid line indicates data fitted with the least squares method. We obtained the SRCLS for different sizes of FOV by fitting this data through the least squares method. In order to avoid the bias of SRCLS at one FOV, the average value of SRCLS at different

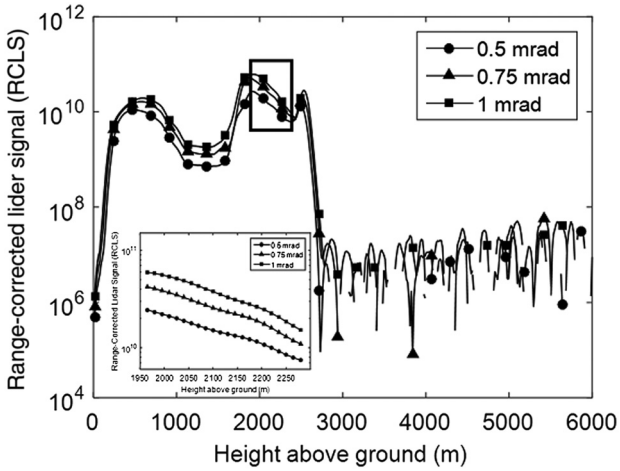

Fig. 5 Lidar signal versus distance from the ground for different sizes of FOV observed by the MFOV Lidar over the northern suburb of Nanjing in East China. Inset: RCLS versus distance from the ground at different FOV at heights between 1965 and 2280 m. (Date and time: December 24, 2016 at 11:34 UTC).

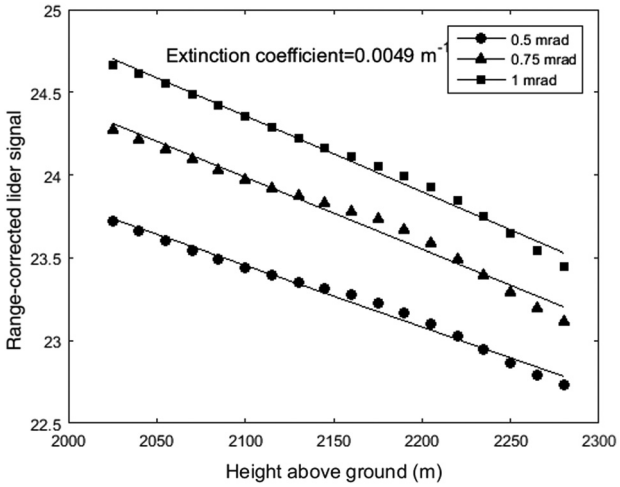

Fig. 6 Extinction coefficient retrieved from SRCLS using data observed from MFOV Lidar. (Date and time: December 24, 2016 and 11:34 UTC).

sizes of FOV was calculated, and the averaged multiple scattering factor η was then calculated based on Eq. (2). From our calculations, the SRCLSs are -0.0037, -0.0043, and -0.0046 m^{-1} when the values of FOVs are 0.5, 0.75, and 1 mrad, respectively, so the average SRCLS is approximately -0.004 m^{-1} and single scattering extinction coefficient is 0.002 m^{-1}.

Thus, CDES can be retrieved from IRCLS by determining the extinction coefficient from SRCLS. Further, Monte Carlo simulation was used to calculate the Lidar signal at different values of FOV for different CDES with our retrieved extinction coefficient. In this simulation, the derived values of SRCLS, CH, CT, and LBD were 0.004 m^{-1}, 1965 m, 2280 m, and 0.4 mrad, respectively, which are obtained from the Lidar signal of measured cloud parameters. Although most parameters used in Lidar measurements and simulations are the same, it is difficult to directly compare the measured data with the simulation data because of the system constants in a real Lidar system. Hence, we need to normalize the observation data to the simulation data with the corresponding FOV. The normalization constant can be expressed as follows:

$$\text{Normalization constant} = \frac{\text{simulated data at one FOV at the cloud base}}{\text{observated data at corresponding FOV at the cloud base}}.$$

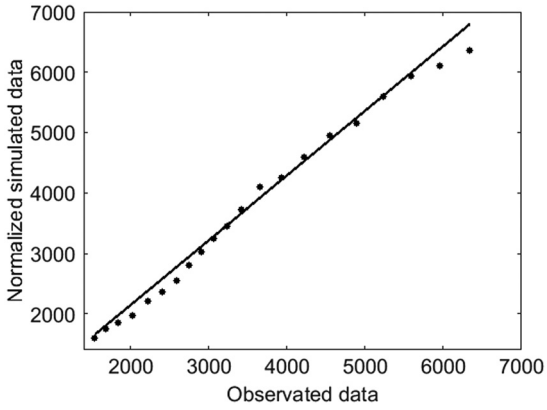

Fig. 7 Observed data versus normalized simulated data at one FOV. (Date and time: December 24, 2016 and 11:34 UTC).

In order to evaluate the consistency between simulated and observed data, we fitted normalized simulated data and observed data by linear regression (solid line, Fig. 7). The goodness of fit can be evaluated by the R^2 value, which is the quadratic power of the correlation coefficient when the two variables are linearly correlated. The correlation coefficient is a measure of the degree of linear correlation between two random variables, defined as follows:

$$r = \frac{\sum_i^n (x_i - \overline{x})(y_i - \overline{y})}{\sqrt{\sum_i^n (x_i - \overline{x})^2 \cdot \sum_i^n (y_i - \overline{y})^2}}, \tag{3}$$

where x_i and y_i are two random variables, $\overline{x}$ and $\bar{y}$ are average values of two random variables, and n is the number of samples. The average R^2 value at different sizes of FOV is calculated for different values of CDES ranging from 21 to 26 μm and at given values of CB, CT, extinction coefficient, and FOV (Fig. 8), where the dotted line indicates R^2 values and the solid line represents the second-order polynomial fitting by the least squares method. The derived second-order polynomial equation is as follows:

$$y = -0.0005079 * x^2 + 0.0746757 * x - 1.7. \tag{4}$$

According to Eq. (4), the R^2 value reaches a maximum when CDES is 23.8 μm.

According to simulated Lidar signal, the average multiple scattering factor η is 0.4097. Following Eqs. (1) and (2), the extinction coefficient of the cloud is calculated as 0.00492 m^{-1}. Figure 9 shows CDES versus LWC with an extinction coefficient of 0.0049 m^{-1}. There is a linear relationship between CDES r_e and LWC w_L at a constant extinction coefficient, which can be written as follows:

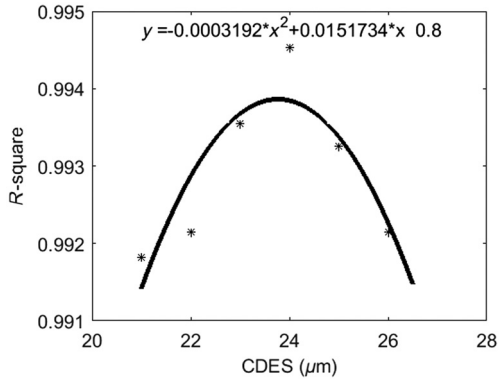

Fig. 8 Averaged R^2 value versus CDES for given values of CB, CT, extinction coefficient, and FOV. (Date and time: December 24, 2016 and 11:34 UTC).

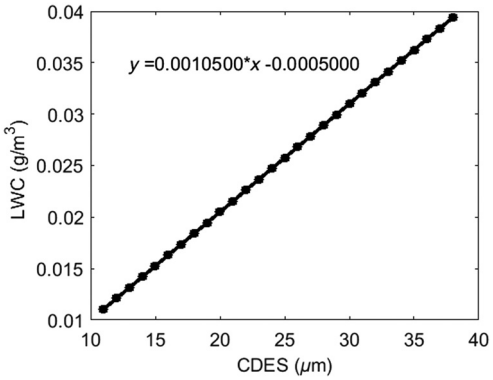

Fig. 9 LWC versus CDES for an extinction coefficient of 0.0049 m^{-1} using data calculated from the Monte Carlo simulation.

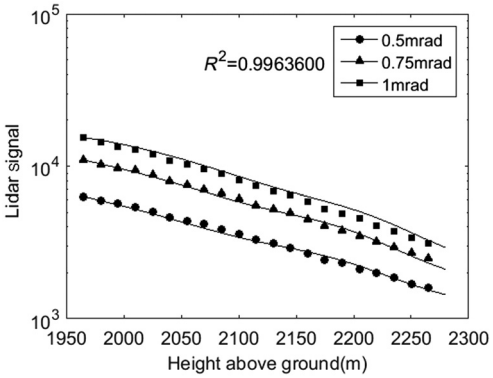

Fig. 10 Lidar signal of observed data and simulated data versus distance from the ground for different values of FOV on a logarithmic scale. (LWC is 0.024 g m^{-3} and CDES is 23.8 μm).

$$w_L = 0.00105 * r_e - 0.0005. \tag{5}$$

As CDES is 23.8 μm, the calculated LWC in this case is 0.024 g m^{-3}. Figure 10 shows the Lidar signal obtained from the observed and simulated data sets versus distance from the ground for different values of FOV on a logarithmic scale, with LWC of 0.024 g m^{-3} and CDES of 23.8 μm. The solid line indicates observed data and the dotted line indicates simulated data. This figure shows good agreement between observed and simulated data.

5 Discussion and Comparison

To verify the accuracy of the algorithm, we compared CDES and LWC measured using this system with the GPM satellite product. The GPM precipitation plan is a new generation of global satellite precipitation product after the Tropical Rainfall Measuring Mission. Its core observation platform was launched on February 28, 2014. The satellite group currently consists of 10 satellites. The GPM Core Observatory is equipped with Dual Frequency Precipitation Radars (DPR) including a Ka-band radar and Ku-band radar. The DPR can provide cloud products such as LWC and a radar reflectivity factor. Hence, we can directly obtain LWC from the DPR onboard the GPM satellite; whereas, CDES can be retrieved from the radar reflectivity factor through Eq. (6):[21]

$$R_e = 50 \exp(-0.5\sigma^2) N^{-1/6} Z_e^{1/6}, \tag{6}$$

where R_e is the CDES of cloud, σ is the assumed logarithmic spread of the droplet size distribution, N is the droplet number concentration, and Z_e is the radar reflectivity factor.

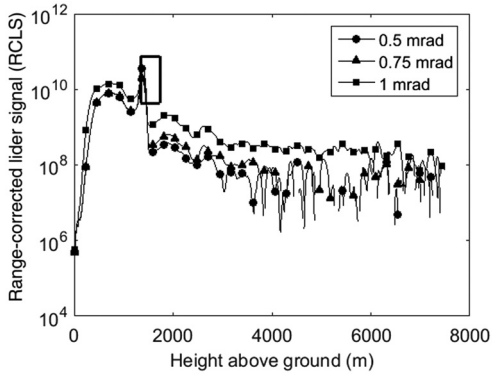

Fig. 11 Lidar signal versus distance from the ground for different values of FOV with data observed by MFOV Lidar. (Date and time: December 10, 2016 and 11:01 UTC).

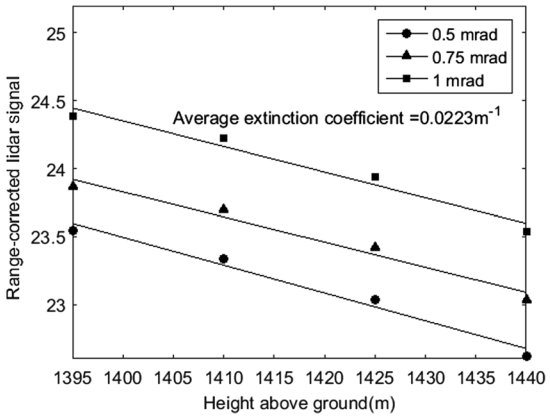

Fig. 12 Extinction coefficient retrieved from SRCLS with data observed from the MFOV Lidar. (Date and time: December 10 2016 and 11:01 UTC).

According to Ref. 21, σ and N are assumed to be 0.31 and 25 to 35 cm^{-1}, respectively. Therefore, a droplet number concentration of 30 cm^{-1} is used in this study.

According to the satellite orbit, we made observations when the satellite passed through Nanjing (32.2 N, 118.719E) on December 10, 2016 (Fig. 11), and the CB was ~1395 m and the CT was ~1440 m (the first layer). Hence, we extracted data from 1395 to 1440 m to calculate the LWC and CDES of the Lidar signal. Because the cloud is thin in this case, we just get four-point valid data for the regression analysis. Figure 12 shows the extinction coefficient calculated for this case. The average extinction coefficient and multiple scattering factor η were calculated using the above method; the average extinction coefficient is 0.0223 m^{-1}. Because the extinction coefficient calculated in this case was much larger than that in the former case, it more likely cause multiple scattering. CDES was also calculated based on the MFOV Lidar. From our calculations, the derived second-order polynomial equation of CDES and R^2 is as follows:

$$y = -0.002 * x^2 + 0.1928 * x - 3.7736. \tag{7}$$

According to Eq. (7), the average CDES calculated from MFOV Lidar is ~48.2 μm. The corresponding CDES retrieved from the radar reflectivity factor that can be obtained directly from the GPM product is shown in Fig. 13, where the black circle represents the location of Nanjing, which is the closest distance to our observation station. In this figure, the CB is ~1400 m, which is almost the same as that derived from the MFOV Lidar. It is also evident that the cloud is inhomogeneous, as the LWC is not the same at different longitudes and altitudes. This difference may cause bias between the MFOV Lidar and GPM. CDES is ~50 μm at the

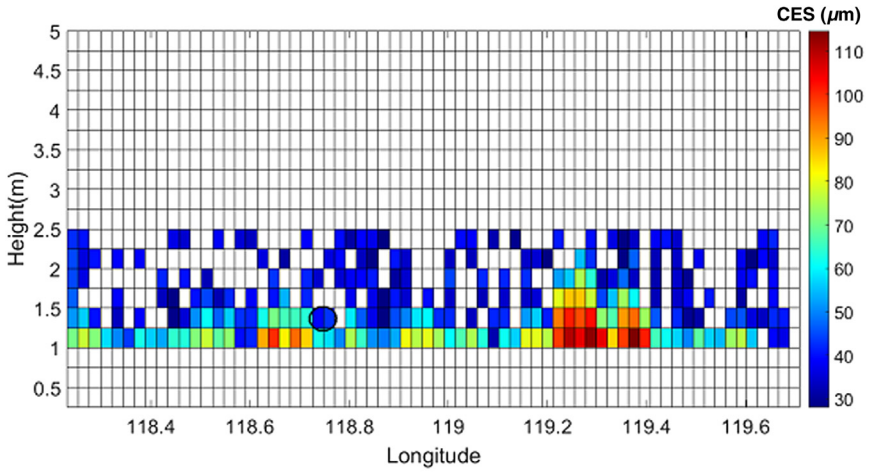

Fig. 13 CDES retrieved from radar reflectivity factor obtained from the GPM product. (Date and time: December 10, 2016 and 11:01 UTC).

corresponding longitude and altitude. The measured CDES also shows reasonable agreement between the MFOV Lidar and GPM.

Based on the aforementioned method, the LWC is also derived from MFOV Lidar using a value of 0.26 g m^{-3}. The LWC obtained from the GPM is shown in Fig. 14, where the black circle represents the location of Nanjing and the LWC is ~0.1 g m^{-3}. The LWC obtained from the GPM and Lidar is not consistent. However, the LWC and CDES values should follow Eq. (8):

$$\mathrm{LWC} = \frac{2}{3} r_{\mathrm{eff}} * \alpha * \rho, \tag{8}$$

where α is the extinction coefficient for single scattering, r_{eff} is the CDES, and ρ is the water density. The deductive process is demonstrated in Eqs. (9)–(11), as shown in Ref. 14:

$$\alpha = \int_0^\infty n(r) Q_{\mathrm{ext}} \pi r^2 \mathrm{d}r \approx \int_0^\infty n(r) 2\pi r^2 \mathrm{d}r, \tag{9}$$

$$\mathrm{LWC} = \frac{4}{3} \rho \pi \int_0^\infty r^3 \mathrm{d}r, \tag{10}$$

$$r_{\mathrm{eff}} = \frac{\int_0^\infty n(r) \mathrm{r}^3 \mathrm{d}r}{\int_0^\infty n(r) \mathrm{r}^2 \mathrm{d}r} = \frac{\frac{\mathrm{LWC}}{\frac{4}{3}\pi\rho}}{\frac{\alpha}{2\pi}} = \frac{3}{2} \frac{\mathrm{LWC}}{\alpha \cdot \rho}, \tag{11}$$

where r is the cloud droplet size and Q_{ext} is the extinction efficiency, which is approximately equal to 2 when the size parameter $x(= 2\pi r/\lambda)$ is greater than 1. According to our calculations for this case, the extinction coefficient for single scattering $\alpha = 0.0096$ m^{-1}. The CEDS value is 48.2 and 50 μm for the Lidar and GPM results, respectively. Assume that CES is 50 μm, according to Eq. (11), the LWC is 0.3 g m^{-3}, which is closer to the Lidar result (0.26 g m^{-3}); thus, the CDES retrieved from the MFOV Lidar and GPM show reasonable agreement, while the LWC values obtained from the two techniques are not in agreement; however, the result retrieved from the MFOV Lidar is more reasonable based on the theoretical calculations. The obtained bias may be caused by the following situations: (i) temporal and spatial bias between the observation station and GPM satellite, (ii) a nonhomogeneous cloud, (iii) inconsistent scattering of the cross section between the Lidar and radar, and (iv) bias caused by the empirical formula. Compared with satellite data, the MFOV Lidar is a more effective and accurate tool for measuring the microphysical properties of cloud with high temporal and spatial resolution. Thus, Lidar is more useful for studying liquid cloud as it can measure cloud properties for a long time at the same location.

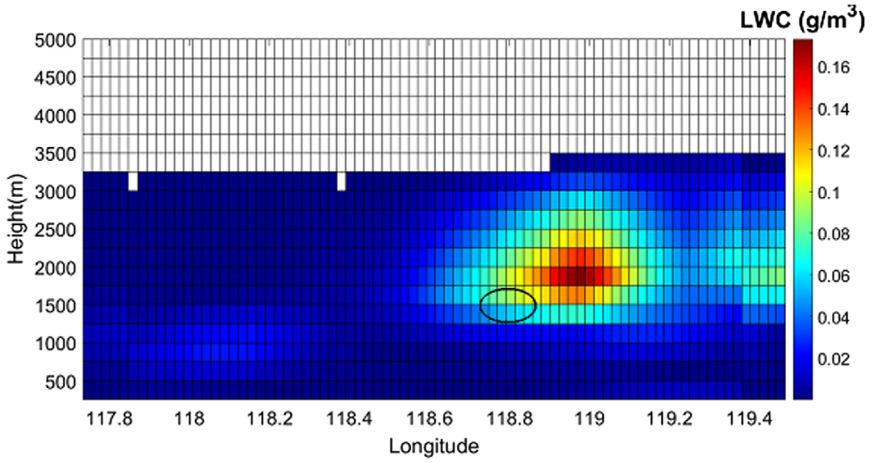

Fig. 14 LWC obtained from the GPM product. (Date and time: December 10, 2016 and 11:01 UTC).

6 Conclusions

A new method for measuring the microphysical properties of homogeneous liquid cloud was proposed based on a Monte Carlo simulation. We conclude that the LWC (or extinction coefficient) and CDES can be extracted using MFOV Lidar by experimentally measuring two independent values: SRCLS and IRCLS. Because the extinction coefficient can be derived directly from SRCLS, it was used to remove ambiguity in the information provided by IRCLS (which varies with both CDES and the extinction coefficient). Once the extinction coefficient was determined, the CDES was extracted from IRCLS at different fields of view, and the LWC was derived from the extinction coefficient using the known CDES. According to the simulation parameters, an innovative MFOV Lidar system was constructed to perform observations of liquid cloud. LWC and CDES were calculated from the observed data based on our proposed method for a case study conducted in the suburb of Nanjing, East China. We also compared LWC and CDES measured by MFOV Lidar with GPM satellite products. This comparison verifies the feasibility of our method for LWC and CDES retrieval during the liquid cloud measurements. This study proposes a new method for measuring LWC and CDES, which can also be used to calculate the size distribution of other particles such as smog or fog.

Acknowledgments

We thank Professor Kim Dukhyeon of Hanbat University, South Korea, for a fruitful discussion of multiple scattering of liquid cloud. This study was partially funded by the National Natural Science Foundation of China (Grant No. 41675133) and the Natural Science Foundation of Jiangsu Province (Grant No. BE2015003-4). The authors declare no conflict of interest.

References

1. A. Sinha, "Effect of atmospheric gases, surface albedo and cloud overlap on the absorbed solar radiation," *Ann. Geophys.* **14**(3), 329–335 (1996).
2. M. Degünther et al., "Effect of remote clouds on surface UV irradiance," *Ann. Geophys.* **18**(6), 679–686 (2000).
3. M. T. Abshaev et al., "Radar estimation of water content in cumulonimbus clouds," *Izv. Atmos. Ocean. Phys.* **45**(6), 731–736 (2009).
4. C. L. Liu et al., "Toward more accurate retrievals of ice water content from radar measurements of clouds," *J. Appl. Meteorol.* **39**(7), 1130–1146 (2000).
5. N. I. Fox et al., "The retrieval of stratocumulus cloud properties by ground-based cloud radar," *J. Appl. Meteorol.* **36**(5), 485–492 (2010).
6. J. Delanoë et al., "Combined CloudSat-CALIPSO-MODIS retrievals of the properties of ice clouds," *J. Geophys. Res.* **115**(D4), D00H29 (2010).

7. D. N. Whiteman et al., "Cloud liquid water, mean droplet radius, and number density measurements using a Raman Lidar," *J. Geophys. Res.* **104**(D24), 31411–31419 (1999).
8. L. Bu et al., "LIDAR and millimeter-wave cloud RADAR (MWCR) techniques for joint observations of cirrus in Shouxian (32.56°N, 116.78°E), China," *J. Atmos. Sol. Terr. Phys.* **148**, 64–73 (2016).
9. J. Schmidt et al., "Dual-field-of-view Raman Lidar measurements for the retrieval of cloud microphysical properties," *Appl. Opt.* **52**(11), 2235–2247 (2013).
10. K. Sassen et al., "Lidar multiple scattering in water droplet clouds: toward an improved treatment," *Opt. Rev.* **2**(5), 394–400 (1995).
11. C. M. R. Platt, "Remote sounding of high clouds. III: Monte Carlo calculations of multiple-scattered lidar returns," *J. Atmos. Sci.* **38**(1), 156–167 (1981).
12. Y. Hu et al., "Global statistics of liquid water content and effective number concentration of water clouds over ocean derived from combined CALIPSO and MODIS measurements," *Atmos. Chem. Phys.* **7**(12), 3353–3359 (2007).
13. Y. Hu et al., "Simple relation between Lidar multiple scattering and depolarization for water clouds," *Opt. Lett.* **31**(12), 1809–1811 (2006).
14. D. Kim et al., "Optical depth and multiple scattering depolarization in liquid clouds," *Opt. Rev.* **17**(6), 507–512 (2010).
15. D. Kim et al., "Measuring cloud droplet effective radius and liquid water content using changes in degree of linear polarization along cloud depth," *Opt. Lett.* **39**(12), 3378–3381 (2014).
16. D. P. Donovan et al., "A depolarisation lidar based method for the determination of liquid-cloud microphysical properties," *Atmos. Meas. Tech.* **8**(9), 237–266 (2014).
17. L. R. Bissonnette et al., "Multiple-scattering Lidar retrieval method: tests on Monte Carlo simulations and comparisons with in situ measurements," *Appl. Opt.* **41**(30), 6307–6324 (2002).
18. S. R. De Roode et al., "The effect of temperature and humidity fluctuations on the liquid water path of non-precipitating closed cell stratocumulus clouds," *Q. J. R. Meteorolog. Soc.* **134**, 403–416 (2008).
19. G. J. Kunz et al., "Inversion of lidar signals with the slope method," *Appl. Opt.* **32**(18), 3249–3256 (1993).
20. D. M. Winker, "Multiple scattering effects in clouds observed from LITE," *Proc. SPIE* **2580**, 60–71 (1995)
21. M. D. Shupe et al., "Deriving mixed-phase cloud properties from Doppler radar spectra," *J. Atmos. Oceanic Technol.* **21**(21), 660–670 (2004).

Hengheng Zhang received his BS degree in optical engineering in 2016. He is pursuing his MS degree at Nanjing University of Information Science and Technology (NUIST). His current research interests include the development of nMFOV LIDAR.

Lingbing Bu received his PhD in optical engineering from the Advanced Laser Technology and Applied Systems Laboratory, Shanghai Institute of Optics and Fine Mechanics, Chinese Academy of Sciences, in 2007. He is a professor at Nanjing University of Information Science and Technology (NUIST). Since 2007, he has been working at NUIST, where his research areas include laser remote sensing, LIDAR technique, and application of LIDAR data.

Haiyang Gao received his PhD in mechanical engineering from Xi'an University of Technology in 2013. He is a lecturer at NUIST, and has been working at NUIST since 2013. His research area includes ground-based airglow imaging interferometer used for detection of wind speed and temperature.

Xingyou Huang is a professor at NUIST. He received his PhD in atmospheric physics from Institute of Atmospheric Physics, Chinese Academy of Sciences in 2002. Since 2002, he has been working at NUIST. His research areas include aerosol and environmental pollution.

K. Raghavendra Kumar is a professor at NUIST. He received the honor of a National Academy of Environmental Science award for junior scientist.